sciendo

DOI: 10.2478/auoc-2025-0012

Ovidius University Annals of Chemistry Volume 36, Issue 2, pp. 103 - 112, 2025

In silico evaluation of the stability and antibacterial activity of some cobalt complexes

Ana-Cristiane DRAGOMIR,[1] Alina Ramona BUZATU,[2] Oana-Raluca POP[*],[3] Mihaiela ANDONI,[3] Doru BUZATU,[4] and Marilena MOTOC[2]

[1]*Doctoral School, Department of Biochemistry and Pharmacology, Faculty of Medicine, Victor Babeş University of Medicine and Pharmacy, 2 Eftimie Murgu Square, 300041 Timisoara, Romania*
[2]*Discipline of Biochemistry, Department of Biochemistry and Pharmacology, Faculty of Medicine, Victor Babeş University of Medicine and Pharmacy, 2 Eftimie Murgu Square, 300041 Timisoara, Romania*
[3]*Faculty of Pharmacy, University of Medicine and Pharmacy "Victor Babeş" Timisoara, Eftimie Murgu Square 2, 300041 Timişoara, Romania*
[4]*National Institute for Research and Development in Electrochemistry and Condensed Matter, Dr. A. Paunescu Podeanu Street 144, 300569, Timisoara, Romania*

Abstract. The properties and stability of six octahedral cobalt(II) complexes were evaluated by means of DFT computations. Three types of ligands were assigned: heterocycles like 1,3-thiazole and 1,2,4-thiadiazole (unsubstituted, and substituted with amine and hydrazine groups, respectively), water molecules and chlorine. The results suggest that the major influence on the chemical properties of the complexes is given by the substituents, and only in a small extent by the heterocycle type. Taking into account the major health issue of the antibiotic resistance, the design of new compounds with antibacterial properties has attracted an increased interest. In this regard, the antibacterial activity of the proposed cobalt complexes has been evaluated by means of molecular docking. Three receptors have been employed, namely *S. aureus* tyrosyl-tRNA, *E. coli* DNA polymerase II, and Methicillin-resistant *S. aureus*, a panthetonate synthetase. The results show that the best results have been obtained for the complexes where the heterocycle is substituted with hydrazine group, followed by the amino-substituted ones.

***Keywords*:** cobalt complex; thiazole; thiadiazole; antibacterial activity; molecular docking.

1. Introduction

Together with the elucidation of the structure of vitamin B_{12}, cobalamin, the interest in cobalt-based compounds has increased. The various forms of cobalamin are necessary for the proper formation of red blood cells, the synthesis and regulation of DNA, and the maintenance of normal brain and nerve function [1-3]. Also, cobalamin is involved in fatty acid and amino acid metabolism. As a result of these biologic activities implications, humans have developed mechanisms to overcome excess cobalt [4, 5]. Given that cobalt is less toxic to humans than platinum, the cobalt-containing compounds are considered a less toxic alternatives to platinum-based cancer drugs [4, 5].

One of the first known cobalt-based drug is Doxovir, a cobalt(III) complex of bis(acetylacetone)-ethylenedimine, with two axially coordinated 2-methylimidazole ligands. This experimental drug exhibits strong microbicidal effects on drug-resistant strains of the herpes virus [6]. Cobalt(II) complexes containing 2,6-bis(2,6-diethylphenyliminomethyl)pyridine showed better cytotoxicities against colorectal adenocarcinoma (HCT 15) and cervical adenocarcinoma (HeLa) cells, with IC_{50} values ranging from 45 to 100 μM. A complex of cobalt(III) with Schiff bases derived from the reaction between salicylaldehyde and ethylenediamine showed moderate activity (IC_{50} < 100 μM) against MCF-7 cancer cells [6]. Cobalt(III) complexes with two ligands [2-(2-hydroxybenzylideneamino)phenol] inhibited HeLa cell growth, but to a lesser extent than cisplatin [6]. Other cobalt coordination complexes, such as those containing bidentate ligands (such as phenanthroline and bipyridine) also show promising *in vitro* activities against cancer cells [6].

Antibacterial and antifungal effects were determined for some octahedral complexes of cobalt(III) with sulfathiazole [7]. The cobalt(III) ion forms a complex with the nitrogen atoms of sulfathiazole molecules that has shown moderate *in vitro* antifungal activity against *A. fumigatus* and *A. flavus*. As an antibacterial agent, the complex showed *in vitro* good activity against *Pseudomonas aeruginosa* [7]. Different biologic activities, including antibacterial, antifungal, anthelmintic and antitumor properties, have been determined for several amphiphilic metal complexes (metallosurfactants) [8]. The structural groups that metallosurfactants usually have in common are long alkyl chains (hydrophobic part) and metal ions that coordinate mainly to nitrogen donor ligands

[*] Corresponding author. *E-mail address:* pop.raluca@umft.ro (Oana-Raluca Pop)

(hydrophilic part) [8]. Other cobalt complexes with antimicrobial activity are cobalt(III) complexes with substituted thiosemicarbazones of 7-hydroxy-4-oxo-4H-chromene-3-carbaldehyde as ligands [9] as well as metal(II) complexes of salicylaldehyde and benzenesulfonyl hydrazone [10]. Antifungal activity has been also reported for new mononuclear cobalt(II) complexes with N-donor ligands like hexamethylenetetramine and meso-tetrakis[4-(benzoyloxy)phenylporphyrin [11].

There are also known a number of cobalt complexes with antitumor role. For instance, the IC_{50} value of substituted pyridoxal N(4)-thiosemicarbazone cobalt (III) complexes showed significant activity against MCF-7 and HeLa cell lines [12]. The complexes demonstrated good cytotoxicity against all cell lines compared to the free ligands, which means that the biological activity is largely attributed to the presence of the central metal ion cobalt(III) [12]. Also, the synthesis and studies on the structure of complexes of colbalt with indomethacin have been reported [13]. The interaction of the metal complexes of indomethacin with DNA and their antioxidant activity give them the possibility to be used in further investigations as potential antitumor agents [13]. Other promising antitumor agents are cobalt and ruthenium complexes with pyrimidine Schiff bases [14], as well as a salen-based cobalt(III) complex that induces apoptosis in Nalm6 cells (leukemia) and BJAB cells (lymphoma) [15]. The complex shows synergistic effects with daunorubicin and vincristine and has a high selectivity towards tumor cells [15].

Several biomedical applications of cobalt were reported, such as cobalt supplements to treat anemia; cobalt nanoparticles as carrier for cytotoxic drugs; radioactive ^{60}Co in different types of cancers [16]. Also, cobalt has applications in dental and orthopedic prosthetics due to its ability to improve the mechanical characteristics as rigidity, but monitorization of potential toxicity of the implants is recommended, as they can release cobalt particles into the body that may lead to thyroid or neurological dysfunctions [16]. Some inorganic compounds have also biomedical applications: cobalt chloride is used by athletes to increase the oxygenation capacity of the blood, while cobalt oxide nanoparticles for treatment of some microbial infections [16]. The cobalt atom is highly toxic for bacteria and fungi because it interacts with their outer membrane and inhibits their enzyme activity and growth.

Cobalt complexes show promise in antibacterial drug design, offering a potential solution to the growing problem of antibiotic resistance. The unique properties of cobalt, such as its multiple oxidation states and diverse coordination geometries, allow for novel mechanisms of action against bacteria. The effectiveness of a cobalt complex as an antibacterial agent depends on its design and great importance is given to the choice of ligands. They can be used to adjust the stability, solubility, and reactivity of the complex. For instance, using ligands that are themselves antibacterial can lead to a synergistic effect, enhancing the potency of the complex.

Thiazole is an essential component in many drugs, including vitamin B_1 (thiamine), antibiotics or antifungals. Also, the thiadiazole core is considered a versatile scaffold in drug discovery due to its ability to modulate various biological pathways and its relatively good liposolubility, which helps it cross cell membranes [17]. Some previous studies of our team members delt with the investigation of different heterocyclic compounds [18, 19]. The amino group basic properties allow it to interact with biological targets such as ion channels and receptors, and it can also be manipulated to influence a drug's absorption, distribution, metabolism, and excretion properties [20]. Several applications are known for the hydrazino group [21, 22], so the theoretical evaluation of metal complexes properties - substituted with the aforementioned groups - may bring useful information regarding the potential biologic activity of the investigated compounds.

Given the continuous interest for the identification of new antibacterial compounds due to the antibiotic resistance issue, the present study deals with the design and investigation of the antibacterial properties of six cobalt(II) octahedral complexes, with thiadiazole and thiazole ligands. Their antibacterial activity has been investigated by means of the *in silico* studies, against three different strains. There will be discussed topics like: (1) the effect of the substituents on the stability and chemical properties of the complexes; (2) the influence of the proposed ligands on ADME properties; (3) identification of the interactions of each proposed cobalt complex with the bacteria strains by means of molecular docking study.

The investigated compounds have the general formula $[CoL_2Cl_2(H_2O)_2]$, where L is the heterocyclic ligand with the following general structure:

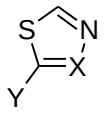

Figure 1. General structure of the ligand **L**

Complex	X	Y
1a	CH	H
1b	CH	NH_2
1c	CH	NH-NH_2
2a	N	H
2b	N	NH_2
2c	N	NH-NH_2

2. Computational details

The structures of the six cobalt complexes were first geometrically optimized at semi-empirical level (PM6 method), and the obtained structures were refined at B3LYP/LanL2DZ level of theory. The geometric optimization of the compounds has been performed with Gaussian 09W software [23]. The same computational program was employed for the calculation of the frontier molecular orbitals HOMO and LUMO energies, as well as the spin density at the cobalt atom (B3LYP/LanL2DZ level of theory).

The global descriptors of reactivity, namely the chemical potential (μ), chemical hardness (η) and

electrophilicity (ω) have been computed by means of equations (1)-(3) [24]:

$$\mu = \frac{E_{HOMO}+E_{LUMO}}{2} \quad (1)$$

$$\eta = \frac{E_{LUMO}-E_{HOMO}}{2} \quad (2)$$

$$\omega = \frac{\mu^2}{2\eta} \quad (3)$$

For the graphic representation of the frontier molecular distribution, as well as for the computation of partition coefficient logP and steric parameters like the Connolly Accessible Area and Connolly Solvent-Excluded Volume, polar surface area and topological diameter, the Chem3D Pro software has been employed. The Multiwfn_3.3.4 software [25] has been employed for the graphic representation of the ELF (Electron Localization Function).

The stability of the cobalt complexes has been also evaluated through the BDE parameter (Bond Dissociation Energy) at B3LYP/LanL2DZ level of theory, using the following reaction:

$$[Co(Het)_2Cl_2(H_2O)_2] \rightarrow Co^{2+} + 2Het + 2Cl^- + 2H_2O$$

$$BDE = E_{Co2+} 2E_{Het} + 2E_{Cl-} + 2E_{H2O} - E_{Complex}$$

In this regard, the structures of the ligands and central cobalt atom were optimized at B3LYP/LanL2DZ level of theory and the obtained energies were employed throughout the calculation.

The ADME properties of the six investigated ligands were computed with SwissADME software [26].

Autodock Vina software [27] has been employed for the evaluation of the antibacterial properties by means of the molecular docking. In this regard, three proteins, namely *S. aureus* tyrosyl-tRNA (1jij.pdb) [28], *E. coli* DNA polymerase II (1q8i.pdb) [29] and Methicillin-resistant *S. aureus*, a panthetonate synthetase (2x3f.pdb) [30] were used as target molecules. Their structures were downloaded in pdb format from the Protein Data Bank of the Royal Society of Chemistry [31]. The following steps have been performed for the preparation of the receptors: (1) the water molecules have been removed; (2) the non-polar hydrogen atoms were not taken into account; (3) the Gasteiger charges have been computed. The proteins were assigned as receptors and a grid box of 40x40x40 Å was used, the center of the grid box being considered the center of the target molecule. Together with the optimized geometries at B3LYP/LanL2DZ level of theory, another geometry optimization of the cobalt complexes has been performed (UFF followed by M06L/TZ2P level of theory), implemented in ADF 2014 software [32]. Two approaches have been employed for the molecular docking: the optimized structures of the complexes were loaded as ligands and the torsions along the rotatable bonds were assigned (flexible ligand docking) and, also, rigid ligand docking (with no internal rotational bonds, using the optimized geometry as input).

The results of the molecular docking study are compared to the ones obtained for Cefazolin, a first-generation cefalosporin. The structure was downloaded from PubChem [33] and subjected to both rigid and flexible molecular docking, without other geometric optimization.

3. Results and discussion

3.1. Characterization of the cobalt(II) complexes

3.1.1. Global and local descriptors of reactivity. The calculation of the global reactivity descriptors for the compounds resulting from the substitution was used to highlight the role of the two substituents $–NH_2$ and $–NH-NH_2$, as well as the heterocyclic skeleton, on the chemical reactivity of the investigated compounds.

Quantum-mechanical calculations can be used to calculate parameters that evaluate the stability and reactivity of the molecular structure. The absolute hardness is calculated by means of the following equation:

$$\eta = \frac{1}{2}(IE - EA),$$

where: IE is the ionization energy, and EA represents the electron affinity.

According to the Koopman theorem, ionization energy can be defined as $IE = -E_{HOMO}$, and the electron affinity $EA = -E_{LUMO}$. A higher energy of the HOMO orbitals corresponds to a higher reactivity in the reaction with electrophiles, while a lower LUMO energy is essential for the reaction with nucleophiles.

The chemical hardness corresponds to the energy difference between the two frontier molecular orbitals and estimates the resistance of a molecule to a change in the electronic distribution.

The global electron affinity can also be used in combination with the ionization energy to calculate another global descriptor of reactivity, the electronic chemical potential (μ), which can be defined as follows: $\mu = -1/2(IE + EA)$

The HOMO (Highest Occupied Molecular Orbital) and LUMO (Lowest Unoccupied Molecular Orbital) energies represent one of the most frequently used molecular descriptors. HOMO energy is directly related to the ionization potential and characterizes the susceptibility of the molecule to an electrophilic attack. LUMO energy is directly proportional to electron affinity and characterizes the susceptibility of the molecule to a nucleophilic attack. The computed HOMO energies show a greater susceptibility to the attack of an electrophilic species for the type **2** complexes, compared with their type **1** analogues.

Table 1. Frontier molecular orbital energies (B3LYP/LanL2DZ)

Complex	E_{HOMO} (a.u.)	E_{LUMO} (a.u.)	Δ (HL gap) (eV)
1a	-0.19877	-0.05065	4.028
1b	-0.18964	-0.05061	3.782
1c	-0.19235	-0.02563	4.535
2a	-0.19434	-0.06843	3.425
2b	-0.19572	-0.04197	4.182
2c	-0.19701	-0.03293	4.463

The distribution of the HOMO orbitals is very similar for all the investigated compounds; for all the complexes, they appear to be localized on the thiazole

and thiadiazole rings. This similarity is also reflected in the close values calculated for the energy of the HOMO orbitals.

Graphical distribution of the frontier molecular orbitals is depicted in Figure 2.

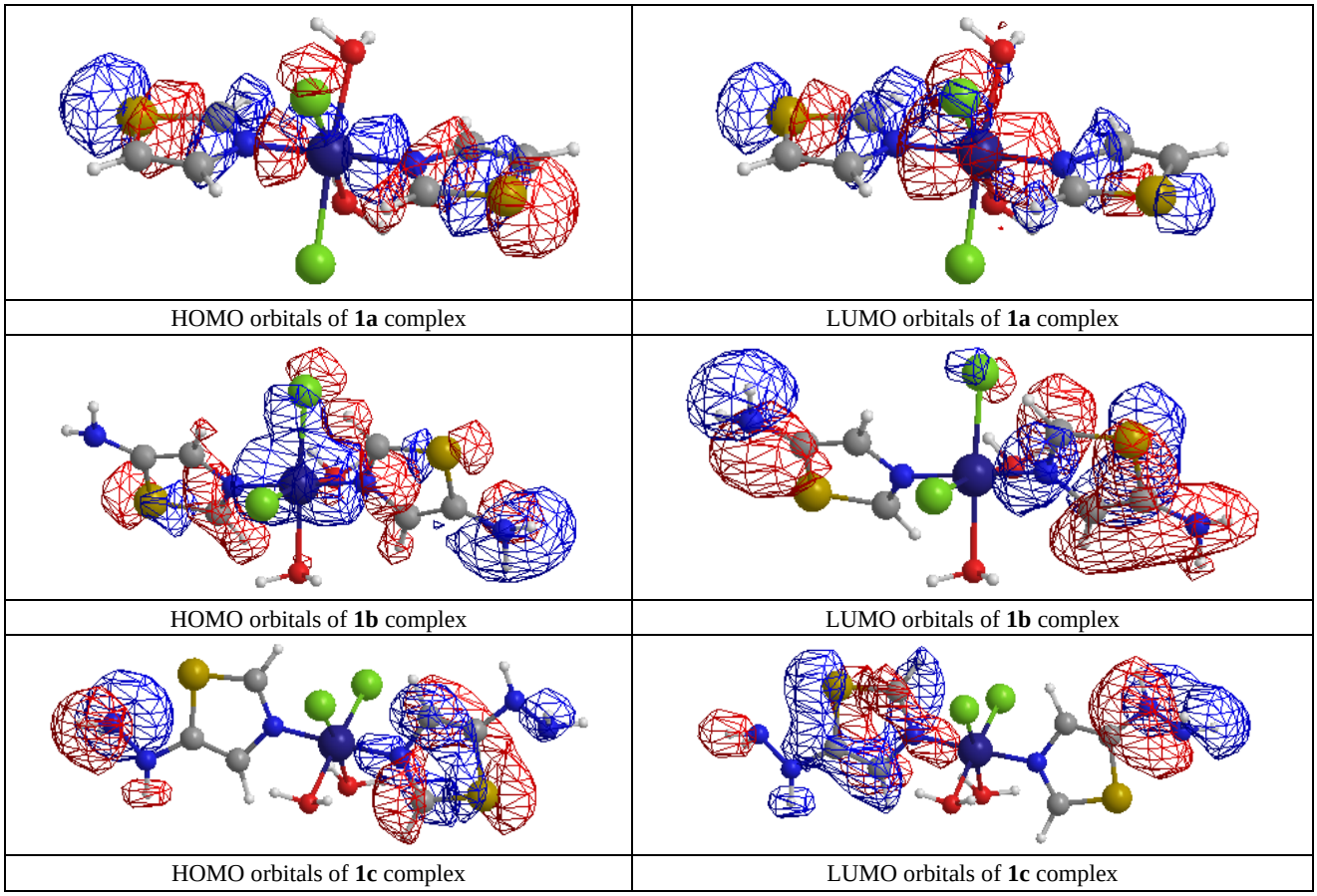

HOMO orbitals of **1a** complex	LUMO orbitals of **1a** complex
HOMO orbitals of **1b** complex	LUMO orbitals of **1b** complex
HOMO orbitals of **1c** complex	LUMO orbitals of **1c** complex

Figure 2. Frontier molecular orbitals of the Co(II) complexes with thiazole ligands

The complexes **1c** and **2c** are also the ones with the lowest values of the LUMO orbitals within the investigated series, and show the same distribution of the orbitals, namely on the heterocyclic ring the hydrazine groups. The lowest values of the LUMO orbitals energies lead also to the lower results of the electrophilicity index, among the investigated complexes. For the complexes **1a** and **1b**, the frontier molecular orbitals LUMO appear mostly localized on the two chlorine atoms; almost equal values of their energies being obtained. Also, these energies are the second highest within the series, following the one calculated for the complex **2a**, where the LUMO appear on both the chlorine atoms and one water molecule.

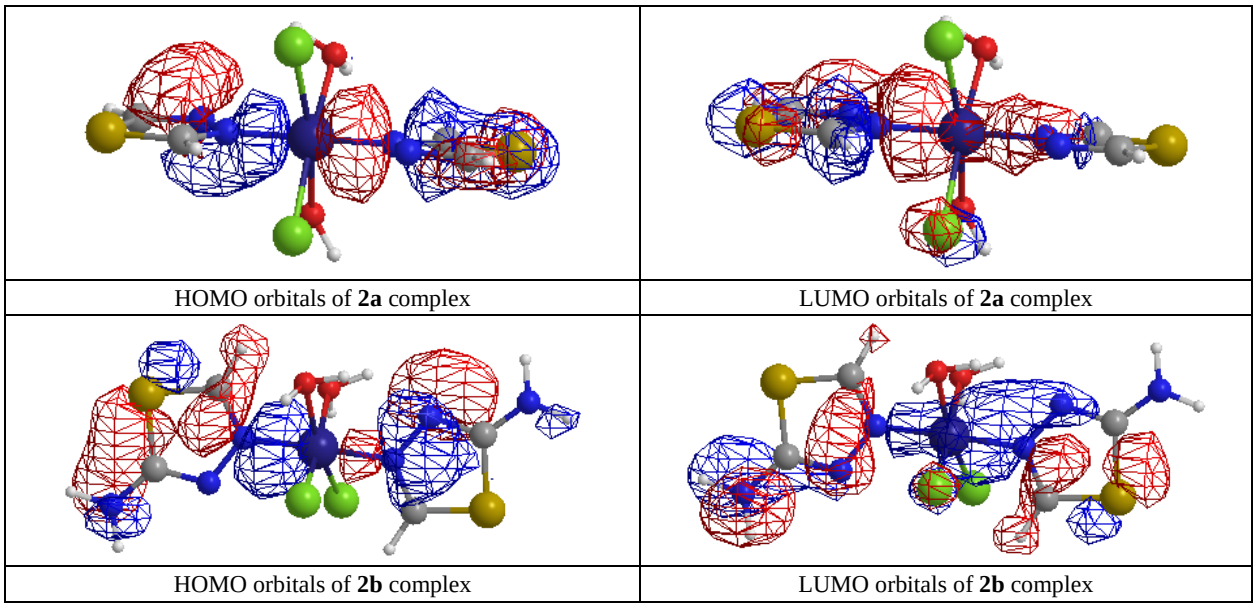

HOMO orbitals of **2a** complex	LUMO orbitals of **2a** complex
HOMO orbitals of **2b** complex	LUMO orbitals of **2b** complex

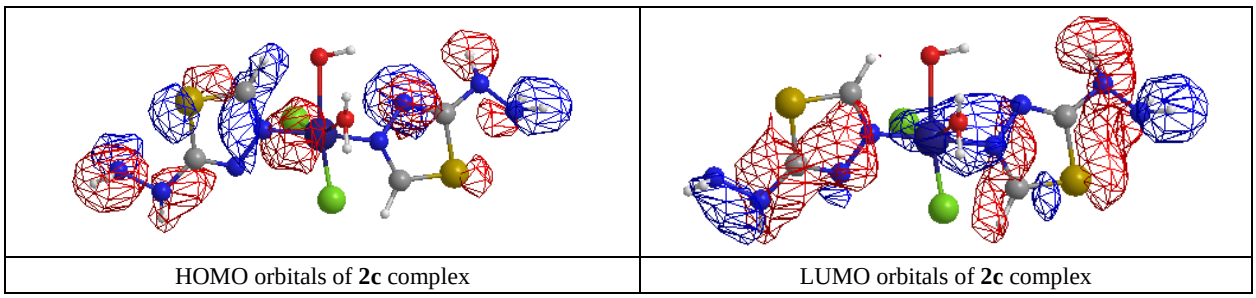

HOMO orbitals of **2c** complex | LUMO orbitals of **2c** complex

Figure 3. Frontier molecular orbitals of the Co(II) complexes with thiadiazole ligands

According to the computed HOMO-LUMO gaps, the most stable compounds are the type **c** complexes, the ones substituted with NH-NH_2 groups. Also, the global reactivity parameters of the complexes have been computed.

Table 2. Global reactivity descriptors of the complexes: chemical potential, chemical hardness, electrophilicity index

Complex	μ (chemical potential) eV	η (chemical hardness) eV	ω (electrophilicity) eV
1a	-3.392	2.014	2.856
1b	-3.267	1.891	2.822
1c	-2.965	2.267	1.939
2a	-3.574	1.712	3.730
2b	-3.233	2.091	2.500
2c	-3.127	2.231	2.192

The lower values of the LUMO energies computed for the type **c** complexes, the ones substituted with –NH-NH_2 groups, are also reflected in the calculated chemical potential and electrophilicity index. The chemical hardness follows the same trend as the HL gap, higher values being obtained for the **1c** and **2c** complexes.

To evaluate the stability of the complexes, the BDE parameter (Bond Dissociation Energy) was calculated. The following general equation was employed for the BDE index calculation:

$$[Co(Het)_2Cl_2(H_2O)_2]^{2+} \rightarrow Co^{2+} + 2Het + 2Cl^- + 2H_2O,$$

where Het = thiazole or thiadiazole, respectively.

Table 3. BDE (Bond Dissociation Energy) parameter computed for the investigated complexes (B3LYP/LanL2DZ)

Complex	BDE (kcal/mol)
1a	764.9
1b	530.8
1c	695.9
2a	754.3
2b	696.5
2c	760.5

According to the above-mentioned results, the most stable complexes are the unsubstituted ones (**1a** and **2a**) and **2c** (thiadiazole ring with hydrazine group), respectively.

In order to evaluate the influence of both the heterocycle and the substituents on the properties of the investigated complexes, the spin density at the cobalt atom and the ELF (Electron Localization Function) have been computed.

The spin densities calculated for the cobalt atom of the six complexes show similar values, regardless the substitution or the heterocycles type.

Table 4. Spin density computed for the Co atom (B3LYP/LanL2DZ)

Complex	Spin density
1a	0.868
1b	0.891
1c	0.885
2a	0.875
2b	0.882
2c	0.871

The graphic representation of ELF (Electron Localization Function) brings important information for the reactivity of compounds; higher values of it indicate regions with a pronounced localization (a covalent bond or a pair of non-participating electrons).

A more pronounced density of electrons is evident around the N and S atoms of the heterocyclic rings, as well as at the central cobalt atom of the complexes.

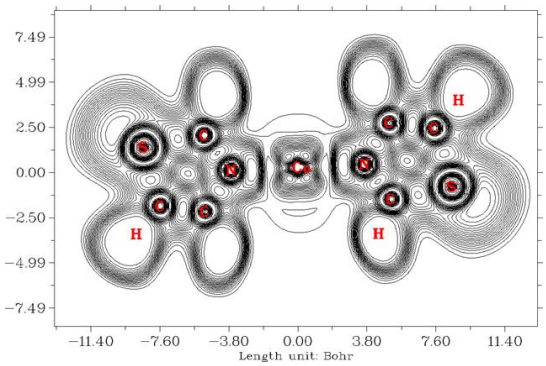

Figure 4. Electron localization function for the complex **1a** (B3LYP/LanL2DZ)

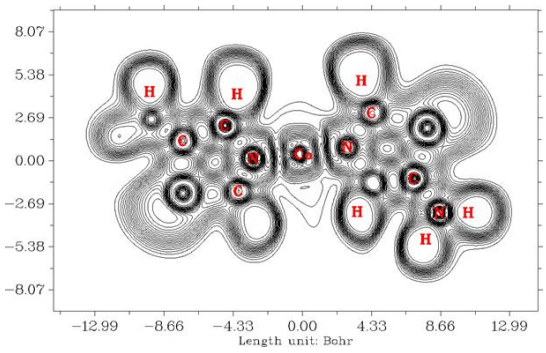

Figure 5. Electron localization function for the complex **1b** (B3LYP/LanL2DZ)

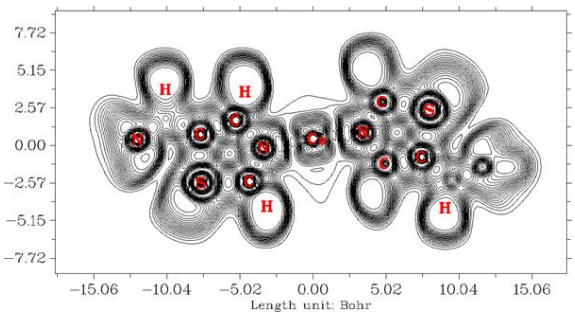

Figure 6. Electron localization function for the complex **1c** (B3LYP/LanL2DZ)

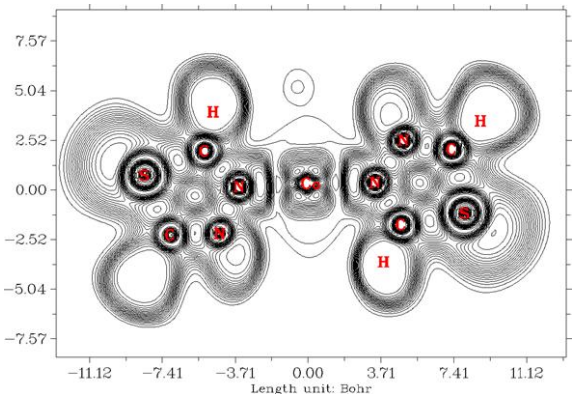

Figure 7. Electron localization function for the complex **2a** (B3LYP/LanL2DZ)

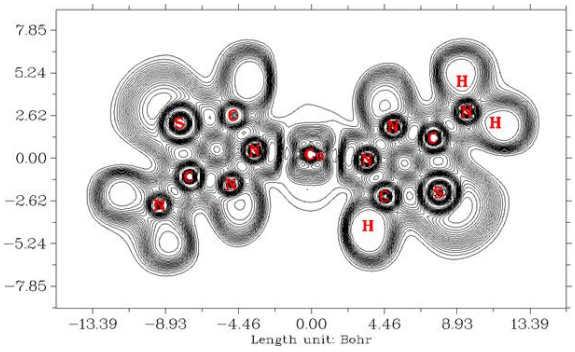

Figure 8. Electron localization function for the complex **2b** (B3LYP/LanL2DZ)

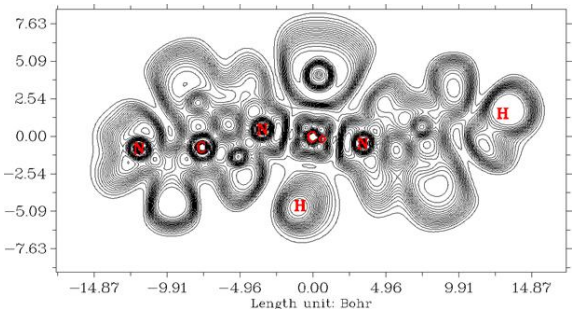

Figure 9. Electron localization function for the complex **2c** (B3LYP/LanL2DZ)

3.1.2. Steric parameters of the compounds. In the field of drug design, molecular shape descriptors are crucial for clarifying the mechanisms of action. The free transfer energy needed to transfer a molecule from an aqueous solvent to a non-polar solvent, like a lipid environment, is frequently determined using the accessible surface. The location of the center of the solvent, as it is rolled over the molecular model, is defined as the Connolly Accessible Area (CAA) [34]. The ovality of a compound quantifies the degree of deviation from the spherical shape [34].

Table 5. Steric parameters of the investigated compound: CAA (Connolly Accessible Area); CSEV (Connolly Solvent-Excluded Volume) and ovality

Complex	CAA (Å^2)	CSEV (Å^3)	Ovality
1a	416.991	191.616	1.294
1b	457.461	210.441	1.341
1c	493.893	228.047	1.383
2a	415.609	188.137	1.297
2b	455.697	205.293	1.356
2c	499.249	224.536	1.404

The results outlined that the major influence is due to the presence of the substituents, larger values being obtained for the compounds substituted with hydrazine groups (type **c**). The nature of the heterocycle does not significantly influence the values of the steric parameters.

Table 6. Number of HBA (Hydrogen Bond Acceptors), HBD (Hydrogen Bond Donors) and partition coefficient (logP)

Complex	HBA	HBD	logP
1a	4	2	1.117
1b	6	4	-0.937
1c	8	6	-0.205
2a	6	2	0.403
2b	8	4	-1.651
2c	10	6	-0.919

As regards the hydrophilicity/hydrophobicity of the complexes, the results outline that the most hydrophobic character has been obtained for the unsubstituted thiazole complex, followed by the unsubstituted thiadiazole one. The presence of the amino group increases the hydrophilic character compared to the hydrazino one, while the presence of the second nitrogen atom within the thiadiazole moiety also leads to a more pronounced hydrophilic character.

Table 7. Polar Surface Area (PSA) and topological diameter (TD)

Complex	PSA (Å^2)	TD (Bonds)
1a	57.60	6
1b	109.64	8
1c	133.70	10
2a	82.32	6
2b	134.36	8
2c	158.42	10

The polar surface area computation reflects the presence of the second nitrogen atom of 2-type complexes in the larger values calculated for the compounds **2a-2c**, compared to **1a-1c**.

3.2. *In silico* evaluation of the biological activity of the metal complexes

The antibacterial activity of the cobalt complexes has been investigated towards three different targets: *S. aureus* tyrosyl-tRNA (1jij.pdb), *E. coli* DNA polymerase II (1q8i.pdb) and Methicillin-resistant *S. aureus*, a panthetonate synthetase (2x3f.pdb).

The antibacterial activity of the cobalt complexes will be compared with the one corresponding to Cefazolin, a first-generation cephalosporin antibiotic. Its

chemical structure is characterized by a central cephalosporin nucleus, with two side chains attached: a tetrazole ring is attached to the β-lactam cycle, while a thiadiazole moiety is attached to the dihydrothiazine cycle.

Table 8. The final Lamarckian genetic algorithm docked state - binding affinities of complexes with the molecular targets (kcal/mol) (**B3LYP/LanL2DZ** geometry, flexible docking (regular)/*rigid docking (italics))*

Complex	***S. aureus* tyrosyl-tRNA**	***E. coli* DNA polymerase II**	**Methicillin-resistant *S. aureus***
1a	-4.52/*-4.90*	-4.85/*-5.24*	-4.38/*-4.76*
1b	-5.08/*-5.76*	-5.60/*-6.11*	-5.16/*-5.56*
1c	-5.59/*-6.15*	-5.88/*-6.60*	-5.81/*-6.30*
2a	-4.63/*-4.91*	-3.49/*-5.11*	-4.36/*-4.57*
2b	-5.19/*-5.70*	-5.52/*-6.12*	-5.03/*-5.56*
2c	-5.73/*-6.17*	-5.96/*-6.56*	-5.83/*-6.06*
Cefazolin	-6.12/	-6.43/	-5.54/

Table 9. The final Lamarckian genetic algorithm docked state - binding affinities of complexes with the molecular targets (kcal/mol) (MO6/TZ2P geometry, flexible docking (regular)/*rigid docking (italics))*

Complex	***S. aureus* tyrosyl-tRNA**	***E. coli* DNA polymerase II**	**Methicillin-resistant *S. aureus***
1a	-4.58/*-4.83*	-5.06/*-5.30*	-4.45/*-4.92*
1b	-5.34/*-5.78*	-5.41/*-6.02*	-5.20/*-5.47*
1c	-5.90/*-6.38*	-5.92/*-6.43*	-5.83/*-6.16*
2a	-4.67/*-4.96*	-4.90/*-5.38*	-4.46/*-4.83*
2b	-5.33/*-5.47*	-5.36/*-6.15*	-5.04/*-5.38*
2c	-5.85/*-6.31*	-5.87/*-6.63*	-5.52/*-6.13*
Cefazolin	-6.12/*-6.87*	-6.43/*-7.23*	-5.54/*-6.83*

For all the three proteins employed as receptors, best binding affinities have been obtained for the type **c** complexes, the ones substituted with hydrazine groups. For the rigid ligand docking, slightly better results are obtained for the cobalt complexes with thiazole ligands, compared to the thiadiazoles. When flexible ligand docking has been performed, thiadiazoles were slightly favored. The results depicted in tables 8 and 9 clearly suggest that better binding affinities have been obtained when the rigid docking method has been employed. The binding energies calculated for the nine conformations of each ligand-receptor interaction are given in the supplementary file (tables S1-S12), together with the graphical representation of the best binding affinity cobalt complex-target protein (figures S1-S12). The compounds **2c** and **1c,** the ones with the highest binding affinities, are also the compounds characterized by the larger Connolly Accessible Area, Connolly Solvent-Excluded Volume and larger polar surface area.

The ligand-receptor interactions, for the best binding affinities, are detailed in tables 10-12.

Table 10. The main interactions of the cobalt complexes with *S. aureus* tyrosyl-tRNA

Complex	Hydrogen bond length (Å) (Donor-acceptor interaction)	Hydrophobic interactions (atoms in close contact)
1a (LanL2DZ)	(1) 1.905 O (H_2O) - [2-amino-3-(4hydroxyphenyl)-propionylamino]-(1,3,4,5-tetrahydroxy-4-hydroxymethyl-piperidin-2-yl)-acetic acid (2) 1.785 O (H_2O) - [2-amino-3-(4hydroxyphenyl)-propionylamino]-(1,3,4,5-tetrahydroxy-4-hydroxymethyl-piperidin-2-yl)-acetic acid (3) 1.995 O (H_2O) – **His47**	Thr42; Lys84; His50;
1b (TZ2P)	(1) 2.182 O (H_2O) – **Asp195**	Leu223; Val224; **His47**
1c (TZ2P)	-	Leu223; **Asp195**; Thr225; Lys226; Phe232; Lys231
2a (TZ2P)	-	Gly49; **His47; Asp195**
2b (LanL2DZ)	(1) 2.771 O (H_2O) - [2-amino-3-(4hydroxyphenyl)-propionylamino]-(1,3,4,5-tetrahydroxy-4-hydroxymethyl-piperidin-2-yl)-acetic acid	**His47**; Ala43; Thr42; His50
2c (TZ2P)	-	**Asp195**; Val224
Cefazolin	-	**Asp195; His50; His47**; Ala43; Val224

Table 11. The interactions of the cobalt complexes with *E. coli* DNA polymerase II

Complex	Hydrogen bond length (Å) (Donor-acceptor interaction)	Hydrophobic interactions (atoms in close contact)
1a (TZ2P)	-	Thr121; **Leu376**
1b (LanL2DZ)	(1) 1.87 N(NH2) – Gly476	Leu488; Glu479; Thr357; Thr121
1c (LanL2DZ)	-	Ile469; Asn472; **Leu376**; Thr357; Pro144
2a (TZ2P)	-	Thr121; Pro144; **Leu376**
2b (TZ2P)	-	Thr121; Pro144; Thr357; Val358
2c (TZ2P)	-	Thr121; Phe119; Arg380; Asn472; **Leu376**
Cefazolin	-	Phe119; **Leu376**; Asn472; Val358

Table 12. The interactions of the cobalt complexes with *Methicillin-resistant S. aureus*

Complex	Hydrogen bond length (Å) (Donor-acceptor interaction)	Hydrophobic interactions (atoms in close contact)
1a (TZ2P)	(1) 1.797 O (H_2O) – Gly124	**Asp127**
1b (LanL2DZ)	(1) 1.932 O (H_2O) – Asp115 (2) 2.012 N (NH_2) – Gly119 (3) 2.135 O (H_2O) – **Asp127**	Ala114; Val110; Lys109
1c (LanL2DZ)	-	Gly102; Pro112; Leu113; Val116; Leu251
2a (TZ2P)	-	Leu61; Gly124; **Asp127**
2b (LanL2DZ)	(1) 1.943 N (NH_2) – Gly119	Ala114; Asp115; Val110; Lys109; **Asp127**
2c (TZ2P)	-	Gln12; **Lys163; Val169**; Asn166; Pro101
Cefazolin	-	Val169; **Val162; Lys163**

Some of the ADME properties have been computed, namely the solubility, gastro-intestinal absorption and the skin permeation coefficient. The results suggest that, except for complex **1a**, all the other five are slightly soluble. High GI absorption has been obtained only for the unsubstituted **1a** and **2a** complexes, while the logKp values suggest a reduced permeation potential for all the compounds.

Table 13. ADME properties of the investigated complexes

Complex	log S	GI absorption	log Kp (cm/s)
1a	-4.17	high	-6.23
1b	-3.18	low	-7.27
1c	-3.00	low	-7.62
2a	-3.28	high	-6.71
2b	-3.86	low	-6.93
2c	-2.91	low	-7.78

Based on the aforementioned results, it may be stated that the cobalt complexes with enhanced antibacterial activity are characterized by the following properties: HOMO-LUMO gap ~ 4.5 eV; ovality ~1.4; Connolly Accessible Area ~ 490-500Å^2; Connolly Solvent-Excluded volume ~225-300 Å^3 (the highest values among the investigated compounds); lopP ~ -1.0. Accordingly, our future studies will pursue the design and characterization of metal complexes with larger values of both HOMO-LUMO gaps and steric parameters.

4. Conclusions

The present study dealt with the *in silico* design and investigation of the chemical properties, stability and antibacterial activity of six cobalt(II) complexes.

According to the computed HOMO-LUMO gaps, the most stable compounds are the complexes of type **c**, the ones substituted with hydrazine moieties, followed by the unsubstituted ones. A greater stability for the c-type complexes is also predicted by the BDE (Bond Dissociation Enthalpy) values. In this case, the lowest stability has been determined for the b-type complexes. As regards the energies calculated for the frontier molecular orbitals, no significant differences have been obtained for the HOMO orbitals; this can be observed in the similar distribution of the above-mentioned orbitals. Differences appear among the LUMO orbitals energies, lowest values being obtained for complexes **1c** and **2c** (thus the larger HOMO-LUMO gaps calculated). These differences among the calculated energy values are also reflected in the LUMO orbitals distribution. For the c-

type complexes, the LUMO orbitals appear at the heterocyclic ring and hydrazine moiety.

The graphical representation of the ELF (Electron Localization Function) outlines that the regions with a higher electron density are the ones around the N and S heteroatoms, and also especially on the amine group of b-type complexes. Most of the atoms in close-contact interactions with the receptors are given by the heterocyclic moieties and the grafted amino groups, the ones with an increased electron density.

The computation of some steric parameters of the complexes like the Connolly Accessible Area, Connolly Solvent-Excluded Volume and ovality, outlines that the main influence on the obtained results is given by the substituent type, not the heterocycles employed as ligands.

The evaluation of the antibacterial activity outlines that highest affinities have been computed towards *E. coli* DNA polymerase II. Type-**c** complexes have given the best results, being the compounds with larger values for ovality, topological diameter and polar surface area. Some of the complexes form hydrogen bonds with different amino acid residues by means of one or both the water ligands; only the N atoms of the amino group (type **b**-complexes) are involved in the formation of the hydrogen bonds. Higher binding affinities are mainly related to an increased number of atoms-in close-contact interactions, rather than depending on the formation of hydrogen bonds. Comparison of the biologic activity of the investigated cobalt complexes to Cefazolin shows an enhanced antibacterial activity of the latter compound. Among the investigated compounds, complexes **1c** and **2c** are the ones with the closest values of their binding affinities. The analysis of the Cefazolin interactions shows amino acid residues common to those of the cobalt complexes: Asp195, His47 and His50, Val224 towards S. aureus tyrosyl-tRNA (1jij.pdb); Phe119, Leu376, Asn472 and Val358 towards E. coli DNA polymerase II (1q8i.pdb); Val169 and Lys163 towards Methicillin-resistant S. aureus, a panthetonate synthetase (2x3f.pdb).

Conflict of interest

Authors have no conflict of interest to declare.

References

[1]. F. O'Leary, S. Samman, Vitamin B12 in health and disease, Nutrients 2 (2010) 299-316. Doi: 10.3390/nu2030299

[2]. E.E. van de Lagemaat, L.C.P.G.M. de Groot, E.G.H.M. van den Heuvel, Vitamin B_{12} in relation to oxidative stress: A systematic review, Nutrients 11 (2019) 482. Doi: 10.3390/nu11020482

[3]. K. Halczuk, J. Kaźmierczak-Barańska, B.T. Karwowski, A. Karmańska, M. Cieślak, Vitamin B12-multifaceted in vivo functions and in vitro applications, Nutrients 15 (2023) 2734. Doi: 10.3390/nu15122734

[4]. G. Genchi, G. Lauria, A. Catalano, A. Carocci, M.S. Sinicropi, Prevalence of Cobalt in the Environment and Its Role in Biological Processes, Biology 12 (2023) 1335. Doi: 10.3390/biology12101335

[5]. D. Osman, A. Cooke, T.R. Young, E. Deery, N.J. Robinson, M.J. Warren, The requirement for cobalt in vitamin B_{12}: A paradigm for protein metalation, Biochimica et Biophysica Acta (BBA) – Molecular Cell Research 1868 (2021) 118896. Doi: 10.1016/j.bbamcr.2020.118896

[6]. M.C. Heffern, N. Yamamoto, R.J. Holbrook, A.L. Eckermann, T.J. Meade, Cobalt derivatives as promising therapeutic agents, Current Opinion in Chemical Biology 17 (2013) 189–196. Doi: 10.1016/j.cbpa.2012.11.019.

[7]. A. Pontoriero, N. Mosconi, L. Monti, S. Bellú, P.A.M. Williams, M. Raimondi, B. Lima, G.E. Feresin, B. Nerli, M. Rizzotto, Synthesis, characterization and biological studies of a cobalt(III) complex of sulfathiazole, Chemico-Biological Interactions 278 (2017) 152–161. Doi: 10.1016/j.cbi.2017.10.004

[8]. C. Schattschneider, S.D. Kettenmann, S. Hinojosa, J. Heinrich, N. Kulak, Biological activity of amphiphilic metal complexes, Coordination Chemistry Reviews 385 (2019) 191–207. Doi: 10.1016/j.ccr.2018.12.007

[9]. G. Kalaiarasi, S. Dharani, S. Rex Jeya Rajkumar, M. Ranjani, V.M. Lynch, R. Prabhakaran, Synthesis, spectral characterization, DNA/BSA binding, antimicrobial and in vitro cytotoxicity of cobalt(III) complexes containing 7-hydroxy-4-oxo-4H-chromene Schiff bases, Inorganica Chimica Acta 515 (2021) 120060. Doi: 10.1016/j.ica.2020.120060

[10]. H.G. Aslan, S. Özcan, N. Karacan, Synthesis, characterization and antimicrobial activity of salicylaldehyde benzenesulfonylhydrazone (*Hsalbsmh*) and its nickel(II), palladium(II), platinum(II), copper(II), cobalt(II) complexes, Inorganic Chemistry Communications 14 (2011) 1550–1553. Doi: 10.1016/j.inoche.2011.05.024

[11]. M. Hajji, N. Amiri, F. Ben Taheur, A. Bujacz, H. Nasri, T. Guerfel, Heteroleptic cobalt(II) complex with nitrogen-rich macrocycles — Structure, bioactivity and DFT modelling, Solid State Sciences 100 (2020) 106117. Doi: 10.1016/j.solidstatesciences.2020.106117

[12]. R. Manikandan, P. Vijayan, P. Anitha, P. Viswanathamurthi, R.J. Butcher, K. Velmurugan, R. Nandhakumar, Synthesis, structure and in vitro biological activity of pyridoxal N(4)-substituted thiosemicarbazone cobalt(III) complexes, Inorganica Chimica Acta 421 (2014) 80–90. Doi: 10.1016/j.ica.2014.05.035

[13]. G.G. Nnabuike, S. Salunke-Gawali, A.S. Patil, R.J. Butcher, M. Lawal, M.O. Bamigboye, J.A. Obaleye, Copper(II) and nickel(II) complexes of the non-steroidal anti-inflammatory drug indomethacin containing aromatic chelating N,N-donor ligand: Synthesis and structural studies, Journal of Molecular Structure 1225 (2021) 129305. Doi: 10.1016/j.molstruc.2020.129069

[14]. M. Caviglia, Z. Li, C. Santini, J. Del Gobbo, C. Cimarelli, M. Du, A. Dolmella, M. Pellei, New

Cu(II), Cu(I) and Ag(I) complexes of phenoxy-ketimine Schiff base ligands: Synthesis, structures and antibacterial activity, Molecules 30 (2025) 1893. Doi: 10.3390/molecules30091893

[15]. S.M. Hopff, L.A. Onambele, M. Brandenburg, A. Berkessel, A. Prokop, Discovery of a cobalt (III) salen complex that induces apoptosis in Burkitt like lymphoma and leukemia cells, overcoming multidrug resistance in vitro, Bioorganic Chemistry 104 (2020) 104193. Doi: 10.1016/j.bioorg.2020.104193.

[16]. Y. Ma, W. Lin, Y. Ruan, H. Lu, S. Fan, D. Chen, Y. Huang, T. Zhang, J. Pi, J.F. Xu, Advances of cobalt nanomaterials as anti-infection agents, drug carriers, and immunomodulators for potential infectious disease treatment, Pharmaceutics 14 (2022) 2351.
Doi: 10.3390/pharmaceutics14112351.

[17]. M. Szeliga, Thiadiazole derivatives as anticancer agents, Pharmacological Reports 72 (2020) 1079-1100. Doi: 10.1007/s43440-020-00154-7.

[18]. M. Andoni, J.M. Pătrașcu, C.A. Dehelean, G.M. Simu, C. Șoica, D. Antal, R. Pop, Comparisons between tridentate bis(benzazoles)-pyridine and bis(benzazoles)triazine ligands: a theoretical study, Croatica Chemica Acta 88 (2015) 241-246. Doi: 10.5562/cca2647

[19]. R. Pop, M. Ilici, M. Andoni, V.N. Bercean, C. Muntean, M.M. Venter, I. Julean, Theoretical considerations regarding the thione-thiol tautomerism in 2-(5-mercapto-1,3,4-thiadiazol-2-ylthio)acetic acid, Acta Chimica Slovenica 62 (2015) 8-14. Doi: 10.17344/acsi.2014.567

[20]. F. Sánchez-Jiménez, M.V. Ruiz-Pérez, J.L. Urdiales, M.A. Medina, Pharmacological potential of biogenic amine-polyamine interactions beyond neurotransmission, British Journal of Pharmacology 170 (2013) 4-16. Doi: 10.1111/bph.12109.

[21]. L. Camaioni, D. Lambert, B. Sendid, M. Billamboz, S. Jawhara, Antifungal Properties of Hydrazine-Based Compounds against *Candida albicans*, Antibiotics (Basel) 12 (2023) 1043. Doi: 10.3390/antibiotics12061043.

[22]. S. Teixeira, E.M.S. Castanheira, M.A. Carvalho, Hydrazides as powerful tools in medicinal chemistry: Synthesis, reactivity, and biological applications, Molecules 30 (2025) 2852. Doi: 10.3390/molecules30132852

[23]. Gaussian 09, Revision B.01, M.J. Frisch, G.W. Trucks, H.B. Schlegel, G.E. Scuseria, M.A. Robb, J.R. Cheeseman, G. Scalmani, V. Barone, B. Mennucci, G.A. Petersson, H. Nakatsuji, M. Caricato, X. Li, H.P. Hratchian, A.F. Izmaylov, J. Bloino, G. Zheng, J.L. Sonnenberg, M. Hada, M. Ehara, K. Toyota, R. Fukuda, J. Hasegawa, M. Ishida, T. Nakajima, Y. Honda, O. Kitao, H. Nakai, T. Vreven, J.A. Montgomery, Jr., J.E. Peralta, F. Ogliaro, M. Bearpark, J.J. Heyd, E. Brothers, K.N. Kudin, V.N. Staroverov, T. Keith, R. Kobayashi, J. Normand, K. Raghavachari, A. Rendell, J.C. Burant, S.S. Iyengar, J. Tomasi, M. Cossi, N. Rega, J.M. Millam, M. Klene, J.E. Knox, J.B. Cross, V. Bakken, C. Adamo, J. Jaramillo, R. Gomperts, R. E. Stratmann, O. Yazyev, A.J. Austin, R. Cammi, C. Pomelli, J.W. Ochterski, R.L. Martin, K. Morokuma, V.G. Zakrzewski, G.A. Voth, P. Salvador, J.J. Dannenberg, S. Dapprich, A.D. Daniels, O. Farkas, J.B. Foresman, J.V. Ortiz, J. Cioslowski, D.J. Fox, Gaussian, Inc., Wallingford CT, 2010.

[24]. J. Padmanabhan, R. Parthasarathi, M. Elango, V. Subramanian, B.S. Krishnamoorthy, S. Gutierrez-Oliva, A. Toro-Labbé, D.R. Roy, P.K. Chattaraj, Multiphilic descriptor for chemical reactivity and selectivity, Journal of Physical Chemistry A 111 (2007) 9130-9138. Doi: 10.1021/jp0718909..

[25]. O. Trott, A.J. Olson, AutoDock Vina: improving the speed and accuracy of docking with a new scoring function, efficient optimization, and multithreading, Journal of Computational Chemistry 31 (2010) 455-461. Doi: 10.1002/jcc.21334.

[26]. T. Lu, F.J. Chen, Multiwfn: a multifunctional wavefunction analyzer, Journal of Computational Chemistry 33 (2012) 580-585. Doi: 10.1002/jcc.22885

[27]. SwissADME: a free web tool to evaluate pharmacokinetics, drug-likeness and medicinal chemistry friendliness of small molecules, Scientific Reports 7 (2017) 42717. Doi: 10.1038/srep42717

[28]. RCSB PDB - 1JIJ: Crystal structure of S. aureus TyrRS in complex with SB-239629 (last accessed 05.05.2025)

[29]. RCSB PDB - 2X3F: Crystal Structure of the Methicillin-Resistant Staphylococcus aureus Sar2676, a Pantothenate Synthetase. (last accessed 05.05.2025)

[30]. RCSB PDB - 1Q8I: Crystal structure of ESCHERICHIA coli DNA Polymerase II (last accessed 05.05.2025)

[31]. RCSB PDB: Homepage (last accessed 05.05.2025)

[32]. ADF 2014, SCM, Theoretical Chemistry, Vrije Universiteit, Amsterdam, The Netherlands.

[33]. https://pubchem.ncbi.nlm.nih.gov/compound/Cefazolin (last accessed 05.05.2025)

[34]. Y. Zyrianov, Distribution-based descriptors of the molecular shape, Jornal of Chemical Information and Modeling 45 (2005) 657-672. Doi: 10.1021/ci050005l

Received: 16.06.2025
Received in revised form: 07.08.2025
Accepted: 03.09.2025